Remote Icing Monitoring and Prediction Model for Icing Accretion on Power Lines

Lou Wenjuan[1], Feng Zhang[1], Chen Yong[1], Wang Qiang[1], Xu Haiwei[1], Huang Mingfeng[1]

[1] *College of Civil Engineering and Architecture, Zhejiang University*

louwj@zju.edu.cn, 21760717@zju.edu.cn, cecheny@zju.edu.cn, 3150105725@zju.edu.cn, haiwei163@163.com, mfhuang@zju.edu.cn

Abstract— **Study of icing on power lines has gained many attentions, because the icing may result in line galloping, flashover and other events that are harmful to the safe operation of transmission lines. And, it still desires effort made to further clarify the intrinsic mechanism of the icing, since the development of the new technology makes it possible to obtain more comprehensive meteorological conditions than before. A remote icing monitoring system on a full-scale power line was setup in the hills in Shengzhou, China, which incorporates an automatic meteorological observation station, ice thickness measuring systems and a video surveillance system. The analysis on the data observed during ice and snow weather in 2018 indicates that the ice thickness is more sensitive to temperature, humidity, precipitation and wind speed than to other parameters. Accordingly, a new model for the prediction of icing accretion is proposed. The comparison of the predicted results and field measurement results shows a good agreement between them.**

Keywords— ***Conductor icing; ice prediction; ice cover growth model; glaze ice; rime***

I. INTRODUCTION

Undesirable loads induced by icing on the power lines, may result in damage of transmission lines, such as flashover, tripping, breakage of conductor, damage of fittings and insulators, even collapse of tower. China is a vast country, and the transmission lines in this county are settled with complex micro-topography and variable microclimate along the transmission lines. For example, at the beginning of 2008, thirteen provinces of China suffered from unusual heavy snowing and serious freezing, which causes a direct economic loss of 23.88 billion RMB [1]. With the development of the power engineering, the icing on power lines brings more and more destructiveness, which leads to higher safety requirements in the design, construction, operation and retaining of power transmission lines. It deserves efforts made to gain insight into the formation and growth of the icing on power lines, which benefits proposing effective prevention and control methods, enhancing the ability to resist the icing on power lines, and strengthening the corresponding research work.

Icing on power lines mainly depends on temperature, wind speed, water droplet diameter and conductor geometry parameters. In general speaking, thermodynamic equilibrium mechanism, fluid mechanics mechanism, environment, conductor current and electric field are involved with the formation of icing [2]. Since the 1950s, extensive studies on icing conductors were carried out, and various models based on relevant meteorological data were put forward to predict the icing accretion. It is found that the empirical formulas in the previous studies are capable of providing a fine simulation. However, most of the studies merely simulate the icing accretion on the conductor within a duration in which the environment condition is unchanged. Accordingly, one may achieve a good result for a short term observing, whereas the deviations from the estimation to the observation becomes greater, because the changing of icing speed are occasionally observed due to the changing actual meteorological condition.

In this paper, a remote icing monitoring system on a full-scale power line setup in the hills in Shengzhou, China, is introduced firstly. The monitoring system incorporates an automatic meteorological observation station, ice thickness measuring systems and a video surveillance system. After a careful survey of the models with corresponding empirical formulas in the previous studies, the valid boundary conditions of the models are summarized. A new methodology for the prediction of icing on power lines is thus proposed, based on the idea of classifying icing stages, namely dividing a long term into time segments. In each stage, the results are computed by using a corresponding appropriate model. The validation of the approach is verified by the results obtained the remote icing monitoring system.

II. CLASSIFICATION OF ICING ON TRANSMISSION LINES

Generally, cold droplets of water falling in the atmosphere are captured and condensed when they hit the conductor that has a temperature of below zero ^{o}C, which in turn form ice layers. According to the meteorological condition in the icing, also the shape of the ice, the ice covering the power lines falls into five categories: glaze ice, soft rime, hard rime, mixed rime and snow. Fig. 1 shows the various types of ice and the characteristics of corresponding icing.

Glaze ice refers to pure transparent ice with a density of 0.8~0.9 g/cm^3, and it is of tight texture and strong adhesion. In the area with a low altitude and a temperature of about -2~2 ℃, glaze ice conventionally results from the formation of cooling raindrops or drizzle landing on the objects below 0 ℃. In mountainous areas, the glaze ice results from the ice crystals that come from the clouds, as well as the ground fog containing atmospheric droplets, on condition that the temperature is about -5~0 ℃ and wind speed is about 5~15 m/s. Glaze ice is the most harmful to transmission lines.

The mixed rime refers to opaque (milky) or translucent ice, usually formed by the interlaced transparent and opaque ices. It has a density of 0.6～0.8 g/cm^3, and is of compact texture and strong adhesion. In the area with a low altitude and a temperature of about -5~1 ℃, mixed rime results from the ice crystals that come from the clouds, or the ground fog containing raindrops. In mountainous areas with temperature

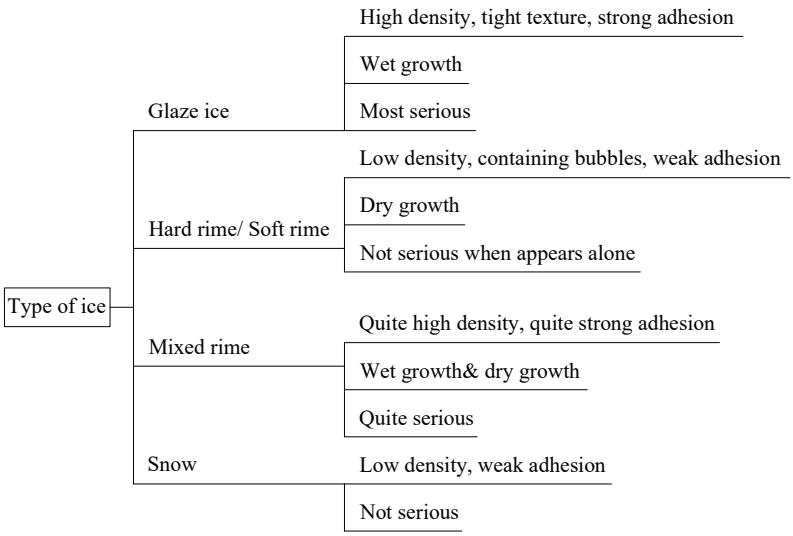

Fig. 1 Types and characteristics of ice on conductors

of -10~-3℃, it results from the ice crystals, or the ground fog containing medium-sized water droplets. Its harm to transmission lines is second only to glaze ice.

Soft rime and hard rime are a white ice that forms when the water droplets in the fog or mist freeze to the surface of objects. Hard rime is formed by supercooled water liquid droplets in the fog with a high wind speed, whereas soft rime is formed by the direct deposition from water vapour to solid ice with calm and light wind. Due to the rapid freezing of water droplet in attaching the object, the air is not easy to escape, so an opaque ice containing extensive small bubbles and holes is formed. Consequently, they have features of loose texture and weak adhesion, and they are fragile and can be easily shaken off objects. Thus the weight of rimes can't be very heavy, and the rimes will not pose a greater threat to the transmission line

III. Remote Monitoring System and Measured Data

A remote monitoring system was developed and implemented to realize a field test of icing on power lines. The system includes a weather monitoring system, a dynamic response monitoring system and an ice shape observation system and it can record simultaneously environmental actions and response data of transmission lines. The monitoring system was applied to a real transmission line across over mountains in Zhejiang province, China. The monitoring target is a span laid between tower 1 and 2 as shown in Fig.2.

Fig. 2 Location of transmission line.

The monitoring system was set up in a weather station located on an 800 m high mountain top below the target span, as shown in Fig.3.This location has complex meteorological conditions, namely perennial low temperature and high humidity, which results in icing easily and a long icing time. It is an ideal experimental base for ice prevention and disaster mitigation of transmission lines.

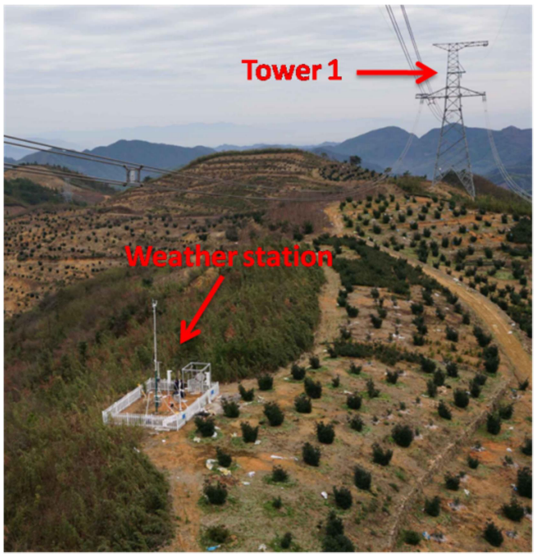

Fig. 3 Weather station.

Fig.4 shows the layout of the weather station. As we can see, there is an aero-elastic segment model which is primarily designed to simulated ice-shedding response of real transmission lines. The segment model consists of a 2 m (width) × 2 m (depth) × 3 m (height) rigid frame, a 2 m long 4-bundled real conductor which was connected to the rigid frame through 4 vertical and 4 horizontal springs, as shown in the Fig.5. The springs were chosen to meet the dynamic similarity between the prototype line and scaled model. The model response under real ice-wind environment can be captured by the camera 1, which was then applied with image recognition technique to derive time history displacements of the conductor model. The front and back camera 2 and 3 in Fig.4 are used to record the ice accretion process, based on which the 3-D ice shape can be

reconstructed using image recognition technique. There is also an ice shape observation frame which is 3m high with two 2m long conductor on its top as shown in the Fig.6 and it is used to collect iced shape considering wind direction effects. In the weather station, a weather monitoring system comprising a wind cup (see Fig. 7), an ultrasonic anemometer (see Fig.8), a thermometer and two rain gauges (see Fig.9) was established to acquire real-time wind, temperature and rainfall information. The wind cup and the ultrasonic anemometer were set at the heights of 10m and 3m, respectively.

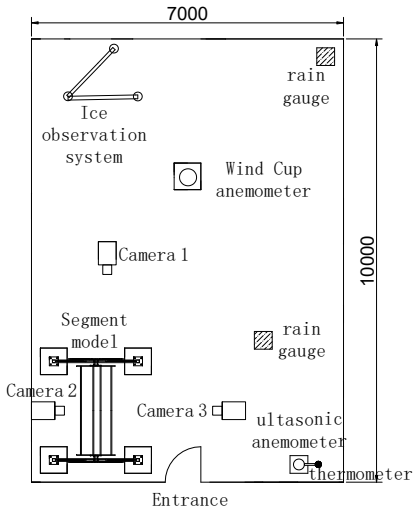

Fig. 4 Layout of weather station.

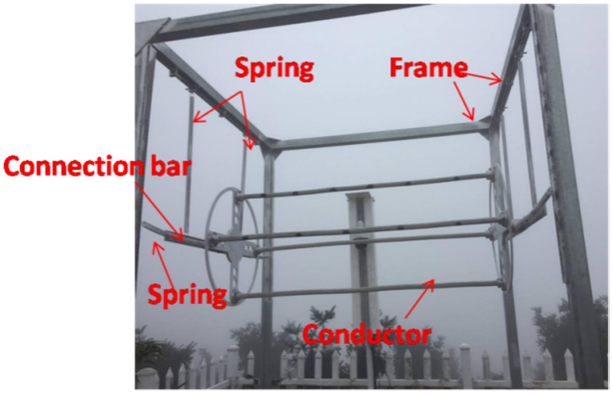

Fig. 5 Segment conductor model.

Fig. 6 Ice observation frame.

Fig. 7 Wind cup anemometer.

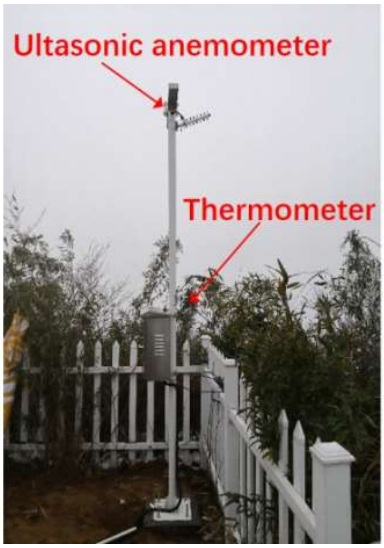

Fig. 8 Ultrasonic anemometer.

Fig. 9 Rain gauge.

To study real transmission line response under joint action of ice-shedding and wind, a set of dynamic response monitoring system was installed on the target line between tower 1 and 2. It contains four acceleration sensors which were mounted at 1/4 span of the target line and 2 tension sensors which were connected to the insulator string, as shown in the Fig.10. The acceleration sensor was installed on

a plate connected to the spacer. Fig. 11 demonstrates installation details of acceleration sensor.

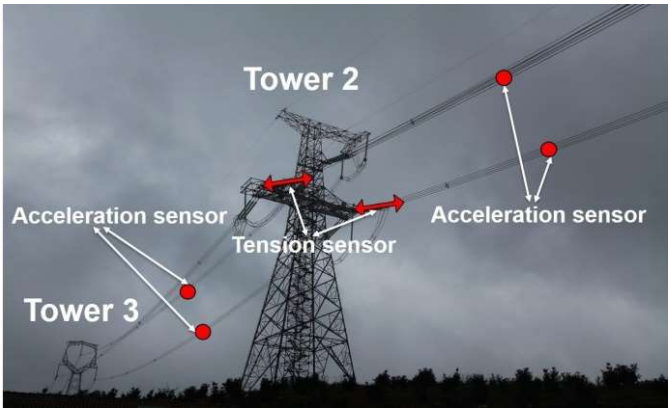

Fig. 10 Monitoring devices on actual transmission line.

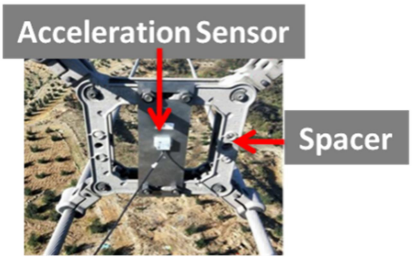

Fig. 11 Installation details of acceleration sensor.

Through the monitoring system, the meteorological parameters and surrounding environment are monitored online in real time. The meteorological data are sampled every minute, and the values of each meteorological element for one minute are obtained by statistics. The icing data are sampled every two minutes. The observational items include equivalent icing thickness, two-minute wind speed and direction, ten-minute wind speed and direction, precipitation, temperature and relative humidity. The time histories of the equivalent thickness of ice, along with the corresponding meteorological parameters are illustrated in Fig. 12, within the duration of from January 10, 2018 to February 5, 2018. It is found that the continuously icing due to the decreasing temperature and raining results in a significant increase of the ice thickness.

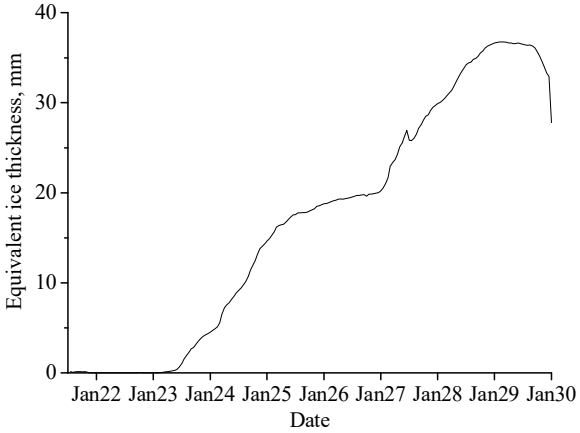

(a) Equivalent ice thickness

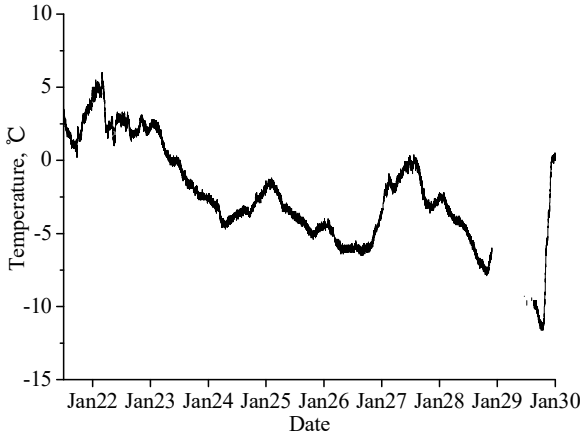

(b) Temperature

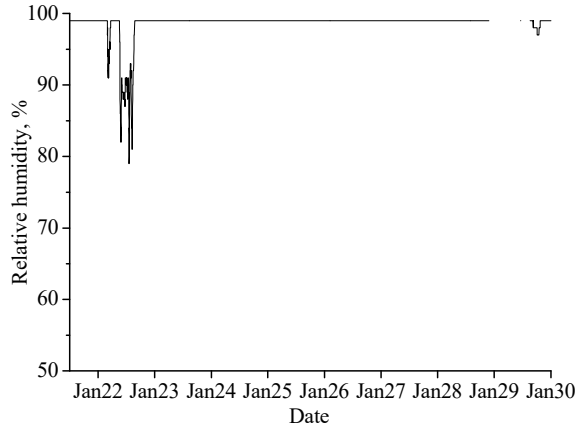

(c) Relative humidity

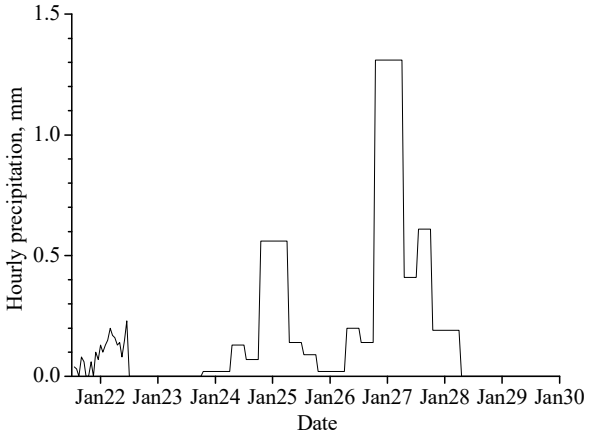

(d) Hourly precipitation

Fig. 12 Time history of equivalent ice thickness and partial meteorological parameters.

IV. Establishment of a New Model

Actually, the mechanism of icing on power lines is very complicated. In previous studies, a variety of models with corresponding calculation formulas were proposed for the prediction of conductor icing using meteorological data. The models are in different forms, and there will be a big difference between the results in predicting the ice thickness using the same meteorological conditions, due to the different hypotheses employed, and the different empirical values of the coefficients adopted, and the slight

inconsistency in choosing relevant meteorological parameters [3].

Many recent studies were carried out based on five models: Lenhard model [4], Imai model [5], Goodwin model [6], Chaine model [7] and Makkonen model [8]. For example, Deng et al. [9] put forward an hourly standard ice thickness model based on conventional meteorological data, where the growth, retaining and shedding of ice can be hourly discriminated. Moreover, the formulas in the model can be used to calculate the ice accumulated hourly. Based on the approaches by Liu et al. [3] and Chen et al. [10], a discriminant process is proposed herein and illustrated in Figure 13, in which the synthesis of precipitation, temperature, humidity and wind speed is used. It is believed that the calculation means in this model is really concise, and the parameters utilized in the calculation can be achieved easily.

A. Prediction Model

The whole procedure of the icing and de-icing can be divided into six stages, namely glaze ice/mixed rime deposition, soft rime deposition, hard rime deposition, retaining stage, thermal melting and sublimation. Based on the temperature, precipitation, humidity and wind speed, the stages of the icing can be identified. Thus, the formula for each stage can be utilized individually to calculate the growth rate of the ice.

1) *Retaining Stage*. It is regarded that there is no change in weight of ice.

2) *Glaze Ice/Mixed Rime*. The growth rate of ice weight, $\dot{M}$ in grams per meter per hour, can be computed by using Jones's model [11], i.e.

$$\dot{M} = \rho_i \pi \Delta r_t (\Delta r_t + D_{t-1}) \tag{1}$$

where

$$\Delta r_t = \frac{1}{\rho_i \pi}[(P\rho_w)^2 + (0.2412VP^{0.846})^2]^{0.5} \tag{2}$$

where Δr_t is the growth rate of glaze ice/mixed rime ice thickness in millimetres per hour, $\rho_{i=}0.6$ g/cm^3 is the density of ice, $\rho_{w=}1.0$ g/cm^3 is the density of water, P is the precipitation rate in millimetres per hour, V is the two-minute average wind speed in meters per second, D_{t-1} is the diameter of ice-covered power line in previous step in millimetres.

3) *Hard/Soft Rime*. $\dot{M}$ can be computed based on the Makkonen's model [12-13], i.e.

$$\dot{M} = 3.6\alpha_1\alpha_2\alpha_3 QVD_{t-1} \tag{3}$$

where Q is the liquid water content in the air in g/m^3, α_1 is the collision rate, α_2 is the collection rate, and α_3 is the freezing rate. For the liquid water content at different temperature, interpolation can be used. The theoretical approach for calculating α_1 and α_2 is really complicated. In this paper, the product of α_1 and α_2 is defined as a collection coefficient, E, by using the equation proposed by Liu et al. [14]. It is in a form of

$$E = (1+108.7D_e/\mathrm{Re})^{-1.05} \tag{4}$$

where D_e=D/d in which D is the diameter of the ice-covered power line with an initial value of 33.6 mm, d is the median diameter of the droplet and has a value of 30μm. Re=VD/v is Reynolds number, and v=1.45×10^{-5} m^2/s is the kinematic viscosity of air. Calculation formula proposed by Chen et al. [15] for α_3 is

$$\alpha_3 = \frac{-(h+\sigma a)T + \frac{h\varepsilon L_e}{c_p p_a}(e_0 - e_a) - \frac{hrV^2}{2c_p} - Fc_w T}{F(\lambda - 1)L_f} \tag{5}$$

where T is the temperature in Celsius, F=QV is the quality flux of liquid water in air, λ = 0.3, L_f is the freezing latent heat of water, h is the convection heat exchange coefficient, and h=kN_u/D in which k is the air thermal conductivity and N_u=0.032Re$^{0.85}$ [14] is the Nusselt number relative to circular motion of airflow, σ=5.67×10^{-8} W·m$^-$2·K^{-4} is the Stefan Boltzmann constant, a=8.1×107 K^3. ε=0.622, L_e is the evaporation latent heat of water, c_p is the fixed pressure specific heat of dry air, p_a is the ambient atmospheric pressure, e_0 and e_a are the saturated water vapor pressure above ice and the ambient air water vapor pressure respectively, r=0.79 is the local recovery coefficient, c_w is the specific heat of water. According to the work by Liu and Hu [16], e_0 can be estimated by

$$e_0 = 6.1e^{22.51-6149.28/(T+273.15)} \tag{6}$$

where e is the natural constant.

In calculating the increment of the ice thickness, the density of the hard rime is chosen to be 0.3 g/cm^3, and the density of soft rime ice is chosen to be 0.1 g/cm^3.

4) *Thermal Melting*. The empirical formula by Farzaneh et al. [17] is utilized, and $\dot{M}$ can be computed by

$$\dot{M} = -87 - 80T \tag{7}$$

in which T is the Celsius temperature in the corresponding stage.

5) *Sublimation*. The reduction in ice weight can be computed by [17]

$$\dot{M} = -7 \tag{8}$$

B. Predicted and Measured Results

In order to reduce the error in prediction, constant α_3 for the initial 12 hours is set, namely α_3=0.2 in the first six hours of icing and α_3=0.1 in the next six hours. After that, α_3 is always computed via Eq. (5).

Considering that the relatively high liquid water content in the air that is caused by the special micro-topography and micro-meteorological conditions in the target area, will have a greater impact on the predicted results, it is necessary to carry out the sensitivity analysis of icing to liquid water content in the air. Define

$$Q_a = Q/\chi \tag{9}$$

where Q_a is the liquid water content in the air related to the air temperature, χ is the adjustment coefficient for liquid water content. Both the measured equivalent ice thickness and the predicted ice thickness are shown in Fig. 14 where the value of χ taken for computing Q ranges from 1.0 to 1.5 with an increment of 0.1. It is found that the prediction model can be further optimized by taking an appropriate adjustment coefficient for different stages.

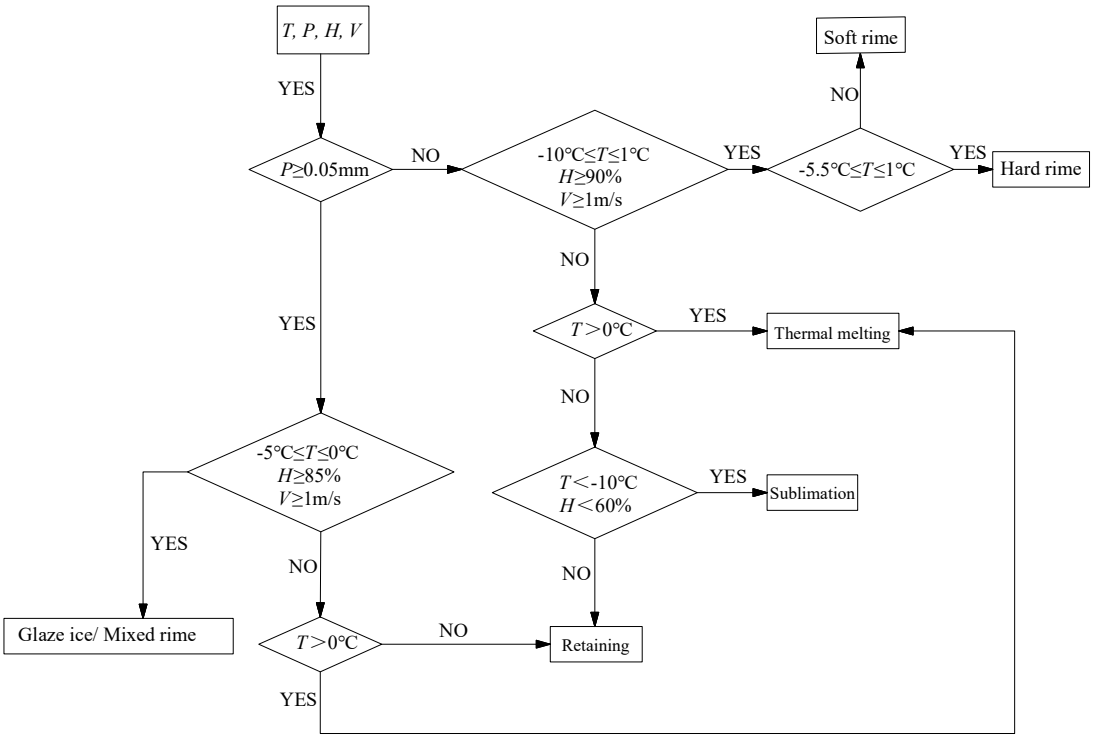

Fig. 13 Discrimination of icing on power lines.

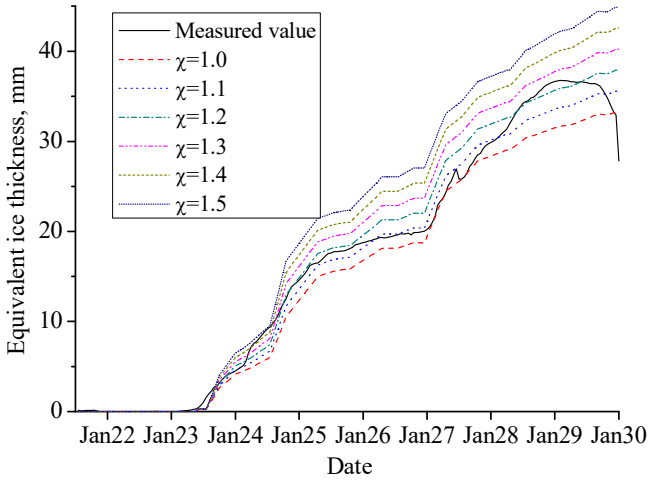

Fig. 14 Numerical results of equivalent ice thickness.

Therefore, using adjustment coefficient is helpful in achieving a better precision. The finally-adopted values of χ are listed in Table 1. Dividing one day into two periods: 0:00-12:00 and 12:00-24:00, the values of mean value, maximum value, and standard deviation corresponding to each period are then obtained, and listed in Table 2. Accordingly, it is found that the results obtained by prediction method agree well with the field test results, which validated the proposed simulation approach.

TABLE I. VALUES OF χ FOP PREDICTION

8: 00 on 23th to 24:00 on 25th	**18: 00 on 28th to 17:00 on 29th**	**Other**
1.2	1.5	1.0

The correspondingly updated time history of the equivalent ice thickness from the predicting formula is illustrated in Fig. 15, along with the field measured results.

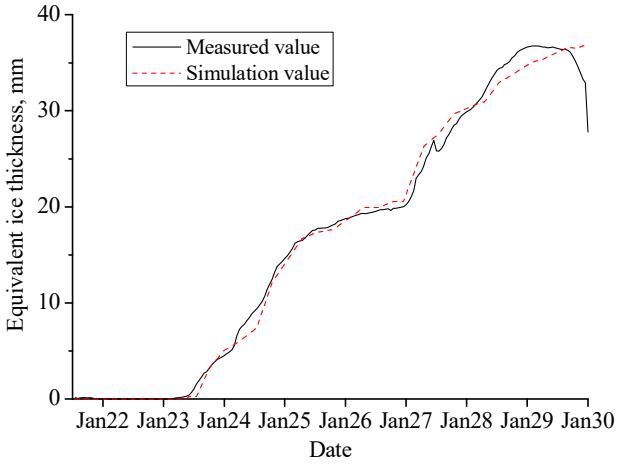

Fig. 15 Calculated and measured ice thickness

V. DISCUSSIONS AND CONCLUSION

Conventional meteorological data which can be easily attained are used in the model. In the prediction, hourly calculating and superimposing are employed, which can intuitively reflects the trend of the developing of ice thickness. Validation of the model is corroborated by field measured results with a good agreement observed.

The uncertainty in the proposed model is mainly attributed to the empirical values of liquid water content in the air, droplet diameter, collection coefficient and freezing coefficient. Besides, when the ambient temperature rises considerably in a short duration, the iced conductor enters a stage of thermal melting, which results in the ice detaching from the conductor suddenly, and consequently the ice-

TABLE II. PREDICTED AND MEASURED RESULTS

Date	Time	Observed			Calculated		
		Mean (mm)	Maximum (mm)	Standard Deviation	Mean (mm)	Maximum (mm)	Standard Deviation
Jan. 22	0:00~12:00	0.08	0.16	0.063	0	0	0
	12:00~24:00	0	0	0	0	0	0
Jan. 23	0:00~12:00	0	0	0.009	0	0	0
	12:00~24:00	0.26	1.05	0.313	0.26	0.07	0.118
Jan. 24	0:00~12:00	3.25	4.52	0.995	5.08	3	1.589
	12:00~24:00	7.02	9.17	1.604	7.23	6.16	0.673
Jan. 25	0:00~12:00	12.16	14.61	1.87	14.08	11.27	2.213
	12:00~24:00	16.48	17.59	0.86	17.25	16.2	0.961
Jan. 26	0:00~12:00	18.16	18.77	0.384	18.57	17.78	0.407
	12:00~24:00	19.22	19.55	0.221	19.94	19.58	0.443
Jan. 27	0:00~12:00	19.84	20.21	0.17	21.28	20.42	0.346
	12:00~24:00	23.93	26.93	2.103	27.41	25.33	1.85
Jan. 28	0:00~12:00	28.05	29.9	1.425	30.25	29.23	0.899
	12:00~24:00	31.92	34.22	1.445	32.63	31.2	0.741
Jan. 29	0:00~12:00	35.58	36.63	0.807	34.77	33.87	0.59
	12:00~24:00	36.65	36.77	0.088	36.09	35.47	0.379
Jan. 30	0:00~12:00	34.59	36.41	2.475	36.86	36.58	0.192

shedding-induced jumping of the conductor. It is rather harmful to the transmission lines. However, in the proposed model, this is not well considered. Indeed, the model assumed that the melting process of ice is slow and continuous, which means that the model is not capable of simulating the ice shedding. It is necessary to perform a further study to eliminate these deficiencies.

ACKNOWLEDGMENT

The authors would like to acknowledge the financial support of National Natural Science Foundation of China (51838012, 51878607) and State Grid Science and Technology Project (5211JY17000X).

REFERENCES

[1] *Technical code for meteorological survey in electric power engineering (DL/T 5158-2012)*, China Electric Power Planning& Engineering Institute Std. 2012. (in Chinese)

[2] C. C. Liu and J. Liu, "Ice accretion mechanism and glaze loads model on wires of power transmission lines," *High Voltage Engineering*, vol.37, pp. 241-248, Jan. 2011. (in Chinese)

[3] H. Y. Liu, D. Zhou, J. P. Fu and S. Y. Huang, "A simple model for predicting glaze loads on wire," *Proceedings of the CSEE*, vol. 21, pp. 44-47, Apr. 2001. (in Chinese)

[4] R. W. Lenhard, "An indirect method for estimating the weight of glaze on wires," *Bulletin of the American Meteorological Society*, vol. 36, pp. 1-5, Jan. 1955.

[5] I. Imai, "Studies on ice accretion," *Researches on Snow and Ice*, vol. 3, pp. 35-44, Jan. 1953.

[6] E. J. Goodwin, "Predicting ice and snow loads for transmission lines," in *First IWAIS*, 1983, p. 267.

[7] P. M. Chaine and G. Casfonguay, "New approach to radial ice thickness concept applied to bundle like conductors," Industrial Meteorology study IV, Environment, Canada, Toronto, Tech. Rep. 74-11, 1974.

[8] L. Makkonen, "Modeling powerline icing in freezing precipitation," *Atmospheric Research*, vol. 46, pp. 131-142, Jan. 1998.

[9] F. P. Deng, L. L. Kang, Y. J. Jiang, J. L. Chu and Y. Liu, "Model and validation of hourly standard ice thickness based on conventional meteorological data," *Journal of Applied Meteorological Science*, vol. 28, pp. 142-156, Mar. 2017. (in Chinese).

[10] B. L. Chen, S. H. Cao and H. Li, "Numerical simulation study on theoretical model of icing on rime wire," *Power Systems And Big Data.*, vol. 21, pp. 73-81, Aug. 2018. (in Chinese)

[11] K. F. Jones, "A simple model for freezing rain ice loads," *Atmos Res.*, vol. 46, pp. 87-97, Jan. 1998.

[12] L. Makkonen, "Modeling of Ice Accretion on Wires," *Journal of Climate and Applied Meteorology*, vol. 23, pp. 929-939, Jun. 1984.

[13] L. Makkonen and E. P. Lozowski, *Atmospheric Icing of Power Networks. Springer Netherlands*, M. Farzaneh, Ed., Quebec, Canada: Springer Netherlands, 2008.

[14] H. Y. Liu, D. Zhou, J. P Fu and S. Y. Huang, "Dimensional analysis of icing collection coefficient of conductor," *Journal of Huazhong University of Science and Technology*, vol. 29, pp. 76-77, Oct. 2001. (in Chinese)

[15] B. L. Chen, X. X. Hu, X. Wu and Z. G. Cheng, "The establishment of meteorological model of rain and rime wire icing based on process discrimination," *Journal of Applied Meteorological Science*, vol. 29, pp. 354-363, May. 2018. (in Chinese)

[16] G. B. Liu and Z. J. Hu, "A new method for calculating the saturated vapor pressure of ice surface," *Weather*, vol. 20, pp. 24-26, Jan. 1994. (in Chinese)

[17] M. Farzaneh and K. Savadjiev, "Statistical analysis of field data for precipitation icing accretion on overhead power lines," *IEEE T. Power Delivery*, vol. 20, pp. 1080-1087, Apr. 2005.